Metals **2015**, *5*, 504-529; doi:10.3390/met5020504

OPEN ACCESS

metals

ISSN 2075-4701

www.mdpi.com/journal/metals

Review

Understanding of the Structural Relaxation of Metallic Glasses within the Framework of the Interstitialcy Theory

Vitaly A. Khonik

Department of General Physics, State Pedagogical University, Lenin St. 86, Voronezh 394043, Russia; E-Mail: khonik@vspu.ac.ru; Tel./Fax: +7-473-2390433

Academic Editors: K. C. Chan and Jordi Sort Vinas

Received: 31 January 2015 / Accepted: 19 March 2015 / Published: 25 March 2015

Abstract: A review of the new approach to the understanding of the structural relaxation of metallic glasses based on the Interstitialcy theory has been presented. The key hypothesis of this theory proposed by Granato consists of the statement that the thermodynamic properties of crystalline, liquid and glassy states are closely related to the interstitial defects in the dumbbell (split) configuration, called also interstitialcies. It has been argued that structural relaxation of metallic glasses takes place through a change of the concentration of interstitialcy defects frozen-in from the melt upon glass production. Because of a strong interstitialcy-induced shear softening, the defect concentration can be precisely monitored by measurements of the unrelaxed shear modulus. Depending on the relation between the current interstitialcy concentration c and interstitialcy concentration in the metastable equilibrium, different types of structural relaxation (decreasing or increasing c) can be observed. It has been shown that this approach leads to a correct description of the relaxation kinetics at different testing conditions, heat effects occurring upon annealing, shear softening and a number of other structural relaxation-induced phenomena in metallic glasses. An intrinsic relation of these phenomena with the anharmonicity of the interatomic interaction has been outlined. A generalized form of the interstitialcy approach has been reviewed.

Keywords: metallic glasses; structural relaxation; Interstitialcy theory; dumbbell interstitials; shear modulus; heat effects; elastic dipoles

---

1. Introduction

The non-crystallinity of glasses defines the excess Gibbs free energy and, as a result, relaxation of their structure towards the states with lower energy upon any kind of heat treatment. In metallic glasses (MGs), structural relaxation is expressed very markedly, leading to significant, sometimes even drastic changes of their physical properties. For instance, it was found long ago that the shear viscosity of a metallic glass at temperatures below the glass transition temperature T_g (far enough from the metastable equilibrium) can be increased by five orders of magnitude as a result of structural relaxation [1]. The kinetics of homogeneous plastic flow at these temperatures can be described as structural relaxation oriented by the external stress [2]. Structural relaxation is known to affect many physical properties of MGs—mechanical (elasticity, anelasticity, viscoelasticity, *etc.*), electrical, corrosion, magnetic and others [3–5]. Since the beginning of the 1980s, it has remained a subject of unabated interest.

However, in spite of decades-long investigations, the microscopic mechanism and related kinetics of structural relaxation remain a highly debated issue. Most often, structural relaxation is interpreted within the framework of the "free volume" approach, which dates back to the ideas of Doolittle [6], Turnbull and Cohen [7,8], and was later conceptually adopted by Spaepen [9] and Argon [10] to MGs. The free volume model was numerously modified to better describe the property changes [5,11–14]. This model has both advantages (e.g., [4,15]) and drawbacks (e.g., [16,17]), which are, however, beyond the scope of the present paper. Our goal is to review a new comprehensive, versatile and verifiable approach to the understanding of the structural relaxation of metallic glasses, which provides a generic relationship between the crystal, its melt and glass produced by melt quenching. This promising approach is based on the Interstitialcy theory suggested by Granato in 1992 [18,19].

2. Background

The approach to structural relaxation of MGs based on the Interstitialcy theory starts from crystal melting. Frenkel in the 1930s suggested that melting occurs through the thermoactivated generation of point defects of a crystalline structure. There are two types of such defects known from the solid state physics—vacancies and interstitials. Frenkel chose the former and developed a vacancy model of melting [20]. The model was numerously modified [21] and gained much popularity. However, a few issues remained unanswered. One of the first doubts was formulated by Slater [22]. Assuming that the entropy of melting is determined by the generation of vacancies, he concluded that the vacancy concentration just before the melting point should be about 50%, which is clearly unrealistic. It is now known that the volume change and entropy per vacancy upon melting do not agree with the experimental values [18,22,23].

According to Frenkel, the second possibility for point-defect-mediated melting is associated with interstitials. However, available information on these defects over a long period of time was largely inadequate. In particular, it was assumed that interstitials occupy the octahedral cavity in the FCC structure (*i.e.*, in the center of the elementary cell). In 1950, Seitz [24] theoretically considered "an interstitial atom which moves by jumping into a normal lattice site and forces the atom that is there into a neighboring interstitial site" and termed it an "interstitialcy". In the beginning of the 1960s, Vineyeard *et al.* [25,26] performed detailed computer simulation of radiation damage of FCC and BCC

metallic lattices and firmly concluded that interstitials "reside in a split configuration, sharing a lattice site with another atom", which is equivalent to Seitz's interstitialcy. By the middle of the 1970s, the split (dumbbell) nature of interstitials (interstitialcies) in different metals with different crystalline structures became quite evident [27]. To date, it is generally accepted that split interstitials exist in all basic crystalline structures and represent the basic state of interstitials in metals [28,29]. An interstitialcy in a molecular-dynamic model of crystalline copper [30] is shown in Figure 1 as an example.

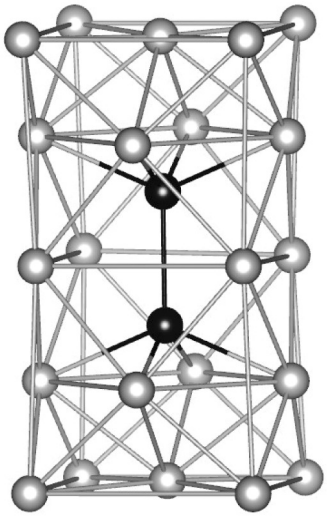

Figure 1. <100> interstitialcy in a molecular-dynamic model of copper [30].

Granato and co-workers made an important contribution to the understanding of the nature of interstitial defects in crystals. In particular, they performed a unique experiment (not repeated so far)—irradiation of a copper single crystal by thermal neutrons at $T = 4$ K with simultaneous measurement of all elastic constants [31,32]. The irradiation results in the formation of long-living (at this temperature) Frenkel pairs. It was found that all elastic moduli decrease with the concentration c of Frenkel pairs, but the shear modulus C_{44} decreases most rapidly. The extrapolation of $C_{44}(c)$-dependence led to the unexpected conclusion that the shear modulus should become zero at $c \approx 2\%$ to 3%. Zero (or very low) shear modulus is characteristic of a liquid [33]. The analysis of the magnitude and orientational dependence of this effect provided the evidence that it is conditioned by interstitial atoms in the dumbbell configuration.

Later, analyzing the thermodynamics of a crystal with interstitialcies, Granato showed that depending on temperature, it is possible to distinguish between several possibilities of stable and metastable equilibrium, which he interpreted as equilibrium/superheated crystal and equilibrium/supercooled liquid states [18,19]. Every stable and metastable state is characterized by its own interstitialcy concentration. Melting of a crystal within the framework of this approach is understood as a result of the thermoactivated generation of interstitialcies, which to a large extent define the properties of the equilibrium and supercooled melt.

This viewpoint is supported by the fundamental property of interstitialcies—the existence of low frequency resonance vibration modes in their vibration spectrum [27,34]. These modes correspond to the frequencies, which are by several times smaller than the Debye frequency. Consequently, the vibrational entropy of the defect becomes large, by several times bigger than that of the vacancy (for Cu, for instance,

$S^{int}/k_B \approx 15$, while $S^{vac}/k_B \approx 2.4$ [35] for interstitialcies and vacancies, respectively, where k_B is the Boltzmann constant). This then allows explaining (contrary to vacancies) the observed entropy of melting $S_m = Q_m/T_m$ (where Q_m is the heat of melting, T_m the melting temperature). Indeed, there is a remarkable empirical Richards rule [36,37], which states that the entropy of melting per atom S_m^{at} for elemental substances is close to $1.2k_B$, with only a few exceptions [37]. Assuming that melting is connected with interstitialcy formation, one can calculate exactly this value for S_m^{at} [23]. The other major finding was that the interstitialcy formation enthalpy rapidly decreases (by several times) with their concentration at large c strongly promoting melting [30,38]. Within the framework of this approach, one can quantitatively explain the empirical Lindemann rule ($\alpha T_m = const$, where α is the crystal thermal expansion coefficient), as well as the correlation between the melting temperature and shear modulus [39].

Thus, the Interstitialcy theory implies that melting can be understood as a result of thermoactivated interstitialcy generation. This is in agreement with earlier results by Stillinger and Weber [40], who performed molecular dynamic simulation of the BCC structure and found that the elementary structural excitations are vacancy-interstitialcy pairs, which define the defect-induced softening and lead to first-order melting. The coexisting solid and liquid are close to defect free and almost maximally defective states. Several other molecular dynamic experiments noted an important role of interstitialcies in melting [38,41–43] and even in the crystallization of simple metals [44]. Recent molecular dynamics work by Betancourt *et al.* [45] makes sense of the interstitialcy in liquids, and the results seem to accord remarkably with defect concentration estimates given by Granato [18,19]. An important result was presented in [38]. The authors concluded that the "string" atoms, which were repeatedly noticed in computer simulations of supercooled liquids and glasses [46,47] and said to resemble the signatures of interstitialcies in crystals [48], have many of the same properties as interstitialcies in crystals, and these properties become even closer as the interstitialcy concentration approaches a few percent. The idea that the liquid state has an interstitialcy concentration of about a few percent [18] has led to a successful interpretation of property peculiarities for equilibrium and supercooled liquids [23,49].

If the hypothesis on interstitialcy-mediated melting has real meaning and interstitialcies indeed retain their individuality in the molten state, then one simply comes to the conclusion that the glass prepared by freezing of melt should also contain interstitialcies, as indeed suggested by computer simulations of amorphous copper [30,38,50]. Another support for this hypothesis comes from the fact that many features of low-temperature glass anomalies (low-frequency vibrations, relaxation processes and general two-level system behavior) are also observed in crystals after irradiation (which produces vacancy-interstitialcy pairs) at doses much lower than those needed for amorphization [51]. Besides that, the volume dependence of the shear elastic constant associated with radiation-induced disordering and eventual amorphization was found to be virtually identical to that associated with heating up to the melting point [52]. However, it is likely that interstitialcies in liquid and glassy states (while keeping the same or similar properties) do not have direct structural representations, as they do in the crystalline state (see Figure 1).

In any case, if glass contains interstitialcies, its structural relaxation upon heat treatment should be conditioned by a change of the interstitialcy concentration. It is this idea that is analyzed and tested below.

3. Interstitialcy-Mediated Structural Relaxation and Related Relaxation of the Shear Modulus

3.1. Relaxation Kinetics

Interstitialcies exert a pronounced impact on the high-frequency (unrelaxed) shear modulus. This is directly stated by the basic equation of the Interstitialcy theory, which suggests an exponential decrease of the shear modulus G of a crystal with the interstitialcy defect concentration c [18,19],

$$G(T,c) = G_x(T)exp(-\alpha\beta c) \quad (1)$$

where $G_x = G(c = 0)$, β is the dimensionless shear susceptibility and $\alpha = \frac{1}{G\Omega}\frac{dU}{dc}$ with U being the internal energy and Ω the volume per atom. Using a numerical fit for copper, Granato found that $\alpha \approx 1$ [18]. Since β is about 15 to 25, Equation (1) implies a strong decrease of the shear modulus with the interstitialcy defect concentration in crystal.

Following the conceptual framework described above, it is natural to assume that Equation (1) should be also valid for glass. In this case, G_x has the meaning of the shear modulus of the reference (maternal) crystal. This assumption leads to rather numerous examples of the successful interpretation of MGs' property changes upon structural relaxation, as reviewed below. The shear modulus within the framework under consideration is the key thermodynamic parameter (as being the second derivative of the free energy with respect to the shear strain [53]) of glass, and precise measurements of G provide an efficient way to monitor the defect concentration and related relaxation kinetics. It is worthy of notice in this connection that the general idea for the key role of the shear modulus in the relaxation kinetics of supercooled liquids and glasses was introduced long ago [54] and currently is gaining increasing acceptance [55–59].

The kinetics of MGs' structural relaxation is intimately related with the state of "metastable equilibrium" [5,60]. While far below the glass transition temperature T_g this state is kinetically unachievable, near T_g it can be reached from opposite sides at reasonable times, leading to different signs of property changes [60]. In particular, this is manifested in the relaxation of the shear modulus G, as illustrated in Figure 2, which gives the temperature dependence of G for bulk glassy $Pd_{40}Cu_{30}Ni_{10}P_{20}$ measured upon linear heating and cooling at the same rate together with the shear modulus G_{eq} in the metastable equilibrium determined by prolonged isothermal tests at different temperatures [61,62]. The temperature T_{pc} in this figure is interpreted as the Kauzmann pseudocritical temperature, *i.e.*, the lowest temperature at which the state of the supercooled liquid is still possible (see [61] for details). At temperatures $T < T_{pc}$, the shear modulus $G < G_{eq}$ (*i.e.*, the current defect concentration c is bigger than the defect concentration c_{eq} in the metastable equilibrium state), and therefore, structural relaxation leads to an increase of G. On the contrary, at $T > T_{pc}$, the shear modulus $G > G_{eq}$ (respectively, $c < c_{eq}$) and structural relaxation decreases it. Different signs of shear modulus relaxation are indeed experimentally observed [63].

It is interesting to notice the shear modulus behavior upon cooling (see Figure 2). Just after switching from heating to cooling, the shear modulus still continues to decrease. This behavior is soon changed into an increase of the shear modulus, but the latter remains significantly smaller than that in the course of the initial heating. Such a big hysteresis turns out to be a characteristic feature of MGs [62]. The obvious reason for it is the big underlying relaxation time [62] (see below Equation (6) and the related discussion).

It should be also emphasized that the shear modulus upon cooling at temperatures $T < T_{pc}$ is quite close the metastable equilibrium (see Figure 2), confirming this state as the limit for the relaxation. Thus, structural relaxation takes place mainly during cooling, contrary to what is usually assumed. Below, we discuss this behavior in more detail (see Figure 4 and related description).

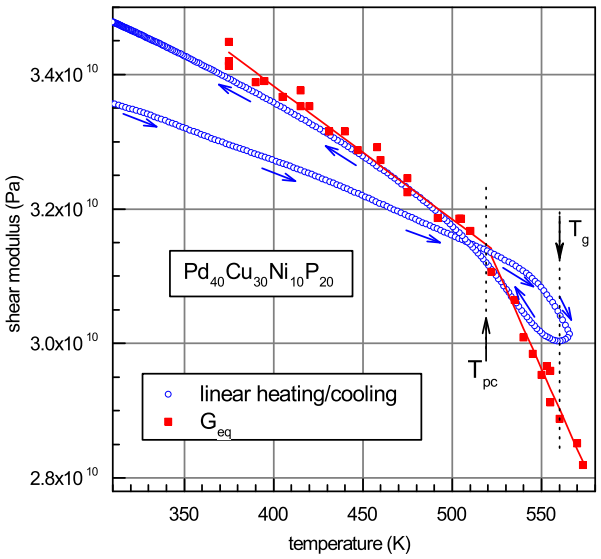

Figure 2. Temperature dependences of the shear modulus for glassy $Pd_{40}Cu_{30}Ni_{10}P_{20}$ upon linear heating and subsequent cooling at a rate of 3 K/min together with the shear modulus in the state of the metastable equilibrium [61,62]. The calorimetric glass transition temperature T_g measured at the same rate is shown by the vertical arrow. The temperature T_{pc} is ascribed to the Kauzmann pseudocritical temperature. The sequence of heating/cooling is given by the arrows.

To analyze the isothermal relaxation kinetics of as-cast glass far below T_g, one can simply consider a spontaneous decrease of the interstitialcy defect concentration, which follows the first-order kinetics. In line with numerous data (e.g., [64]), the corresponding activation energy E should be continuously distributed (e.g., because of the distribution of local shear moduli due to fluctuations in local densities, chemical bonding, *etc.*, as experimentally demonstrated in [65]). Let $N(E,T,t)$ be the temperature-/time-dependent defect concentration per unit activation energy interval. Then, the relaxation kinetics is given by $dN/N = -\nu exp(-E/kT)dt$, where ν is the attempt frequency. If $N_0(E)$ is the initial interstitialcy concentration per unit activation energy interval (*i.e.*, the initial activation energy spectrum, AES), then the time dependence of N after pre-annealing during time τ becomes [66]:

$$N(E,T,t) = N_0(E)exp\left[-\nu(\tau+t)exp(-E/kT)\right] = N_0(E)\Theta(E,T,t) \quad (2)$$

The characteristic annealing function $\Theta(E,T,t) = exp\left[-\nu(\tau+t)exp(-E/kT)\right]$ in Equation (2) sharply increases near the characteristic activation energy $E_0 = kTln\left[\nu(\tau+t)\right]$ and, to a good precision, can be replaced by the Heaviside step function equal to zero at $E < E_0$ and unity at $E > E_0$ [66]. The total concentration c of defects available for relaxation is then given as:

$$c(T,t) = \int_{E_{min}}^{E_{max}} N(E,T,t)dE \approx \int_{kTln\nu(\tau+t)}^{E_{max}} N_0(E)dE \quad (3)$$

where E_{min} and E_{max} are the lower and upper limits of the AES available for activation. Next, for the isothermal test, one can use the "flat spectrum" approximation, $N_0 \approx const$ [66]. Then, the concentration Equation (3) is reduced to $c(t) = N_0 E_{max} - N_0 kTln\nu(\tau + t)$. On the other hand, the basic Equation (1) of the Interstitialcy theory for small concentration changes Δc can be rewritten as $\Delta G(T,t)/G = -\beta \Delta c(T,t)$. Thus, the relaxation kinetics for the relative shear modulus change, $g(t) = G(t)/G_0 - 1$, is given by [67]:

$$g(t) = -\beta \left[c(t) - c_0\right] = \beta kTN_0 ln(1 + t/\tau) \tag{4}$$

Equation (4) at long times $t \gg \tau$ gives the well-known "lnt" kinetics, which is often experimentally observed upon isothermal annealing of as-cast MGs [64,66,68]. In particular, such behavior is documented for the shear modulus change upon structural relaxation far below T_g, even for very long annealing time [67,69]. This is illustrated in Figure 3, which shows a linear growth of g with the logarithm of time after some transient for a Zr-based glass. The red curve gives the fit calculated using Equation (4). It is seen that this Equation gives a good approximation of the relaxation behavior in the range of times from tens of seconds up to about twenty-four hours.

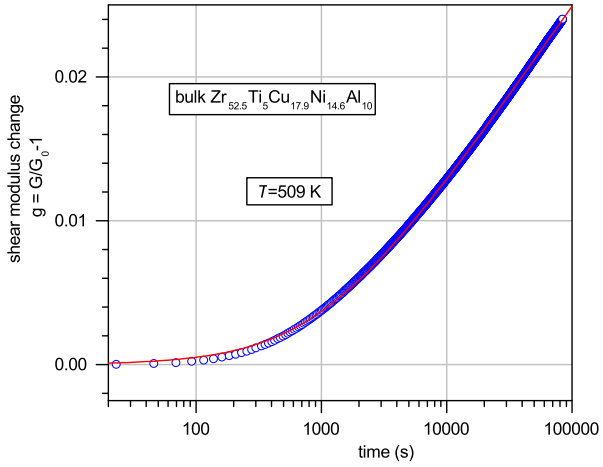

Figure 3. Time dependence of the shear modulus change upon isothermal annealing of bulk glassy $Zr_{52.5}Ti_5Cu_{17.9}Ni_{14.6}Al_{10}$ at $T = 509$ K. The solid red curve gives the fit using Equation (4). Reprinted with permission from American Physical Society, 2008 [67].

The relaxation kinetics upon linear heating can be calculated in a similar way. Since the metastable equilibrium is kinetically achievable at high temperatures, the differential equation for the relaxation should be accepted as:

$$\frac{dc}{dt} = -\frac{c - c_{eq}}{\tau} \tag{5}$$

where c_{eq} is the interstitialcy defect concentration in the metastable equilibrium, which according to Equation (1) has the form $c_{eq} = -\beta^{-1} ln(G_{eq}/G_x)$, with G_{eq} being the shear modulus in the metastable equilibrium.

Using the "elastic" hypothesis for the activation energy of elementary atomic rearrangements [57,58], $E = GV_c$, where V_c is some characteristic volume, the underlying relaxation time can be written down as:

$$\tau = \tau_0 e^{\frac{GV_c}{k_B T}} = \tau_0 e^{\frac{G_0 V_c}{k_B T}(1+\beta\delta c)} = \tau_0 e^{\frac{G_0 V_c}{k_B T}(1+g)} \tag{6}$$

where τ_0 is of the order of the inverse Debye frequency. Then, the relaxation law (5) for heating at a rate $\dot{T}$ can be rewritten as [70]:

$$\frac{dg_{rel}}{dT} = \frac{\gamma - g_{rel}}{\dot{T}\tau_0 exp\left[\frac{G_0 V_c}{k_B T}(1 + g_{rel})\right]} \quad (7)$$

where g_{rel} is the relaxation component of relative change of the shear modulus and $\gamma = \beta c_0(1 - c_{eq}/c_0)$. Equation (7) describes the shear modulus relaxation upon heating at a given rate $\dot{T}$. It was shown that this equation gives a good description of the shear modulus relaxation behavior of bulk glassy $Pd_{40}Cu_{30}N_{10}P_{20}$ at different heating rates, both below and above T_g [70]. The same equation can be used for the interpretation of the shear modulus hysteresis, as illustrated by Figure 4. The bottom part of this figure gives the same shear modulus relaxation data that was shown in Figure 2, but replotted in terms of the relative shear modulus change g (open squares) for temperatures $T > 500$ K. The linear function g_{linf} here represents the $g(T)$-dependence at temperatures below 450 K, where any significant relaxation of the shear modulus is absent. The relaxation part of the relative shear modulus change was then calculated as $g_{rel}(T) = g(T) - g_{linf}(T)$, as given by closed circles in Figure 4. With the appropriate choice of parameters, Equation (7) can be used for the calculation of g_{rel}-dependence, as shown by the red solid/dashed curves. It is seen that, overall, there is quite acceptable correspondence between experimental and calculated shear modulus relaxation data [62], indicating the validity of the approach assumed by Equation (7). It is to be noted that the relaxation time near $T_g \approx 560$ K of glassy $Pd_{40}Cu_{30}Ni_{10}P_{20}$ calculated with Equation (6) is about 2900 s, and it is this large relaxation time that determines the shear modulus hysteresis shown in Figure 4 [62]. It should be also emphasized that the Maxwell relaxation time $\tau_m = \eta/G$ (η is the shear viscosity) at $T = T_g$ is about 20 s, and therefore, the Maxwell viscoelasticity does not constitute a proper basis for the understanding of relaxation phenomena in MGs, even near the glass transition (see [62] for more details).

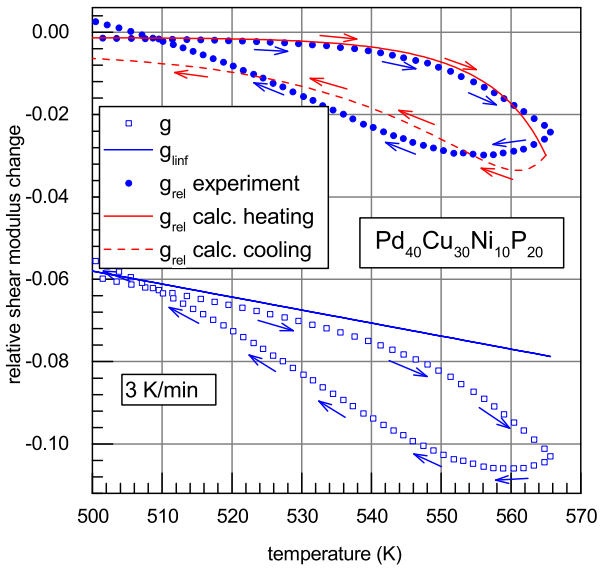

Figure 4. Temperature changes of the experimental relative shear modulus change $g(T)$ for glassy $Pd_{40}Cu_{30}Ni_{10}P_{20}$, its linear approximation $g_{linf}(T)$ for temperatures $T \leq 450$ K together with the experimental and calculated relaxation parts of the relative shear modulus change g_{rel}. The arrows give the sequence of heating/cooling [62].

3.2. Activation Energy Spectra

Upon heating at a constant rate $\dot{T}$, the characteristic activation energy (see above) linearly increases with temperature,

$$E_0 = AT \tag{8}$$

where $A \approx 3 \times 10^{-3}$ eV/K is weakly dependent on $\dot{T}$ and attempt frequency [71]. The shear modulus change then becomes $g(T) = -\beta\left[c(T) - c_0\right]$ with $c(T) = \int_{AT}^{Emax} N_0(E)dE$ and $c_0 = \int_{E_{min}}^{E_{max}} N_0(E)dE$. This gives $g(T) = \beta \int_{E_{min}}^{AT} N_0(E)dE$ and eventually leads to the expression for the AES [67],

$$N_0(E_0) = \beta^{-1}\partial g(E_0)/\partial E_0 \tag{9}$$

The AES for bulk glassy $Pd_{41.25}Cu_{41.25}P_{17.5}$ determined using Equation (9) is given by red triangles in Figure 5, which shows a broad pattern typical of different MGs. This AES starts from the activation energy slightly less than 1.2 eV (this corresponds to temperatures of about 400 K) and ends at activation energies answering to T_g [63,72]. Integration of the AES allows calculating the change of the concentration Δc of defect annealing out upon structural relaxation below T_g. For the AES shown in Figure 5, this gives $\Delta c = 0.00161$, close to the values determined for other MGs ($0.00112 \leq \Delta c \leq 0.00322$ [63,72,73]).

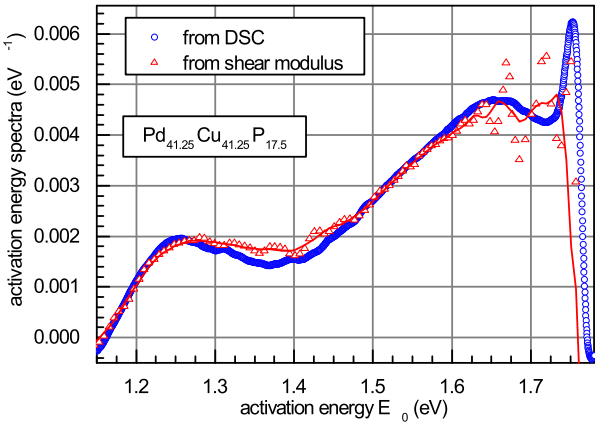

Figure 5. Activation energy spectrum of the structural relaxation of bulk glassy $Pd_{41.25}Cu_{41.25}P_{17.5}$ calculated using shear modulus and DSC data [72].

The full concentration of interstitialcy defects frozen-in upon glass formation can be determined as $c(T) = \frac{1}{\beta} ln \frac{G(T)}{G_x(T)}$ (see Equation (1)). The results of the calculation with this formula for $Pd_{40}Cu_{30}Ni_{10}P_{20}$ glass for a wide temperature range are shown in Figure 6. This figure gives the $c(T)$-dependence for both initial and relaxed (by annealing slightly above T_g) states for the heating rate of 3 K/min together with the metastable equilibrium concentration c_{eq} determined using the metastable equilibrium shear modulus G_{eq} shown in Figure 2. In the initial state, $c \approx 0.0195$ and is nearly independent of T up to temperatures slightly below T_g. At higher T, c rapidly increases, but is still smaller than the equilibrium concentration. At the beginning of the second run, c is smaller by 0.0025 compared to the initial state. This amount is quite close to the values of Δc determined by integration of the AES (see above). On the other hand, the fact that the defect concentration is significantly bigger at the beginning of the second run, but this increase is not seen during the first heating run strongly implies

that structural relaxation takes place mainly upon cooling from the supercooled liquid state during the first heating cycle, as demonstrated by Figure 2. As mentioned above, the plausible reason for this is the big underlying relaxation time [62].

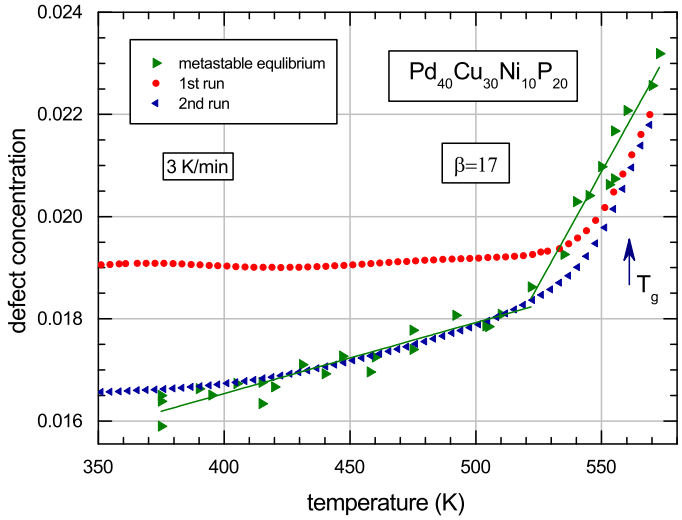

Figure 6. Temperature dependences of the interstitialcy defect concentration for bulk glassy $Pd_{40}Cu_{30}Ni_{10}P_{20}$ in the initial (first run) and relaxed (second run) states measured at 3 K/min together with the metastable equilibrium defect concentration determined from prolonged isothermal shear modulus measurements. The arrow gives the calorimetric glass transition temperature [73].

Thus, within the framework under consideration, the total interstitialcy defect concentration frozen-in upon melt quenching is about 2%, and about one tenth of this amount can be annealed out as a result of structural relaxation. This conclusion is valid for all tested MGs [72,74,75].

4. Interrelationship between the Shear Modulus of Glass, Concentration of Frozen-In Interstitialcy Defects and Shear Modulus of the Maternal Crystal

The basic Equation (1) of the Interstitialcy theory establishes a direct relationship between the shear modulus of glass, the concentration of frozen-in interstitialcy defects and the shear modulus of the maternal crystal. This relationship can be experimentally tested. For this purpose, Equation (1) can be rearranged as:

$$\frac{d}{dT} ln \frac{G_x(T)}{G(T)} = \alpha\beta \frac{dc}{dT} \tag{10}$$

Equation (10) shows that if structural relaxation is absent, *i.e.*, if $c = const$, then the left-hand part of this equation should be zero. Then, one arrives at the equality of temperature coefficients of the shear moduli in the glassy and maternal crystalline states, *i.e.*,

$$\frac{1}{G}\frac{dG}{dT} = \frac{1}{G_x}\frac{dG_x}{dT} \tag{11}$$

Structural relaxation leading to either a decrease of the defect concentration (far below the glass transition temperature) or its increase (near T_g) should result in negative or positive values of the derivative $D = \frac{d}{dT} ln \frac{G_x}{G}$, respectively. These predictions were tested in [73,76].

Figure 7 gives $D(T)$ for $Zr_{46}Cu_{46}Al_8$ glass in the initial and relaxed states (first run and second run on the same sample, respectively) assuming $\alpha \approx 1$. In the initial state, D is indeed very close to zero at temperatures $300 \leq T < 440$ K, reflecting the absence of structural relaxation in this range. At higher temperatures, up to $T \approx 670$ K, D is negative, which corresponds to a decrease of the defect concentration ($\frac{dc}{dT} < 0$, in line with Equation (10)) and the related increase of the shear modulus and heat release [77]. Finally, at $T > 670$ K, D becomes positive and rapidly increases with temperature due to the fast defect multiplication ($\frac{dc}{dT} > 0$), which is manifested in strong shear softening and heat absorption upon approaching the glass transition [77]. In the relaxed state, D is zero up to $T \approx 530$ K again, indicating the absence of structural relaxation. At higher temperatures, D becomes positive and rapidly increases with temperature, suggesting rapid defect multiplication near T_g, which is manifested by strong shear softening and heat absorption [77]. Similar results were obtained on glassy $Pd_{40}Cu_{30}Ni_{10}P_{20}$ [73].

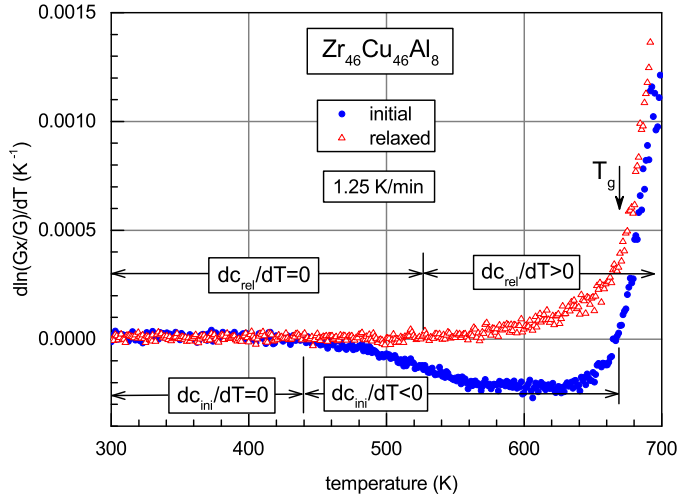

Figure 7. Temperature dependencies of the derivative $\frac{d}{dT} ln \frac{G_x(T)}{G(T)}$ for glassy $Zr_{46}Cu_{46}Al_8$ in the initial and relaxed states. The calorimetric glass transition temperature is shown by the arrow [76].

On the other hand, Equation (11) can be checked directly. Figure 8 shows the ratios of the temperature coefficients of the shear moduli in glassy (initial and relaxed) and crystalline states, $\gamma_{ini} = \left[\frac{1}{G_{ini}} \frac{dG_{ini}}{dT}\right] \left[\frac{1}{G_x} \frac{dG_x}{dT}\right]^{-1}$ and $\gamma_{rel} = \left[\frac{1}{G_{rel}} \frac{dG_{rel}}{dT}\right] \left[\frac{1}{G_x} \frac{dG_x}{dT}\right]^{-1}$, in the temperature ranges where structural relaxation is absent (see Figure 7), and therefore, Equation (11) should be valid. It is seen that both quantities, γ_{ini} and γ_{rel}, are temperature independent and close to unity, supposing a direct relationship between the shear moduli of glass and maternal crystal, as implied by Equation (11).

Thus, the experiments [73,76] described above confirm: (i) the expected relationship between the shear modulus of glass, the concentration of frozen-in defects and the shear modulus of the reference crystal; and (ii) the equality of the temperature coefficients of the shear moduli of glass and the reference crystal in the temperature range with no structural relaxation. Both conclusions validate the basic Equation (1) of the Interstitialcy theory.

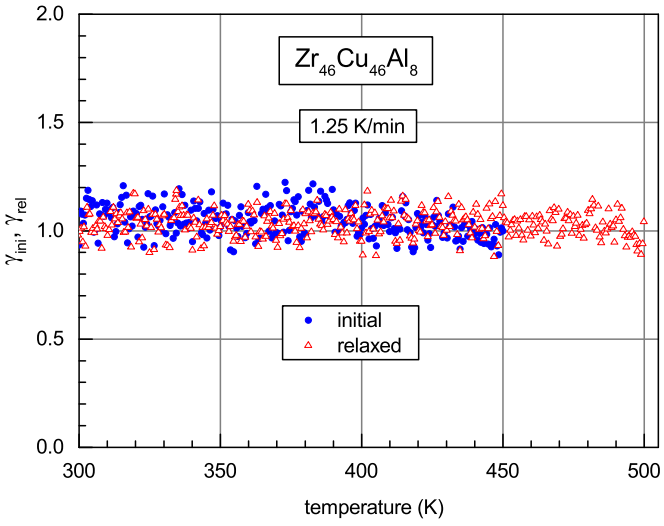

.

Figure 8. Ratios of the temperature coefficients of the shear moduli in glassy (initial and relaxed) and crystalline states of $Zr_{46}Cu_{46}Al_8$, γ_{ini} and γ_{rel}, for temperature ranges where structural relaxation is absent (see Figure 7). Temperature-independent $\gamma_{ini} \approx \gamma_{rel} \approx 1$ confirm Equation (11).

5. Structural Relaxation-Induced Heat Effects

Since there is certain amount of the elastic energy associated with interstitialcy defects, any change of their concentration should lead to heat effects. In particular, annihilation of interstitialcy defects should result in the release of the internal energy in the form of heat. Inversely, interstitialcy defect formation should lead to an increase of the internal energy, which can be revealed as heat absorption. These expectations can be quantified as follows. The formation enthalpy of an isolated interstitialcy is [18,39]:

$$H = \alpha \Omega G \tag{12}$$

where Ω is the volume per atom and G and α have the same sense as in Equation (1). The increment of the number of defects per mole due to an augmentation of their concentration by dc is $dN_d^\mu = N_A dc$, where N_A is the Avogadro number. Then, using Equation (1), the molar interstitialcy formation enthalpy becomes $H_\mu = \alpha \Omega N_A \int_0^c G(c)dc$, and the heat flow occurring upon heating of the molar mass m_μ from room temperature may be found as:

$$W = \frac{1}{m_\mu}\frac{dH_\mu}{dt} = \frac{\alpha \Omega N_A}{m_\mu}\frac{d}{dt}\int_{c_{RT}}^{c} G(c)dc \tag{13}$$

where c_{RT} is the room-temperature defect concentration. Accepting the latter to be $c_{RT} = \frac{1}{\beta} ln\left(G_x^{RT}/G^{RT}\right)$, where G^{RT} and G_x^{RT} are the shear moduli of glass and parent crystal at room temperature, respectively, substituting Equation (1) into Equation (13), one can calculate the heat heat per unit time and per unit mass flow as [78]:

$$W = \frac{\dot{T}}{\beta \rho}\left[\frac{G^{RT}}{G_x^{RT}}\frac{dG_x}{dT} - \frac{dG}{dT}\right] \tag{14}$$

with $\dot{T} = dT/dt$ being the heating rate and ρ the density. It is seen that since G^{RT} and G_x^{RT} are constants, the temperature dependence of the heat flow is simply determined by temperature derivatives

of the shear moduli in the glassy and parent crystalline states. The underlying physical reason consists of the relaxation of the intrinsic defect system.

Figure 9 illustrates the calculation of the heat flow using Equation (14) with $\beta = 17$ in comparison with the experimental DSC runs for bulk glassy $Pd_{40}Ni_{40}P_{20}$ for initial and relaxed (obtained by heating into the supercooled liquid region) states [75]. One can point out a good agreement between calculated and experimental heat release below T_g and heat absorption above T_g. Similar agreement was found for other Pd- and Zr-based metallic glasses [77–79]. Below T_g, a decrease of the interstitialcy defect concentration upon heating leads to the heat release and related increase of the shear modulus. Rapid defect multiplication in the supercooled liquid region (above T_g) requires strong heat absorption and provides a significant decrease of the shear modulus. Moreover, preliminary results indicate that Equation (14) also correctly describes the crystallization-induced heat release relating it with the corresponding relaxation of the shear modulus.

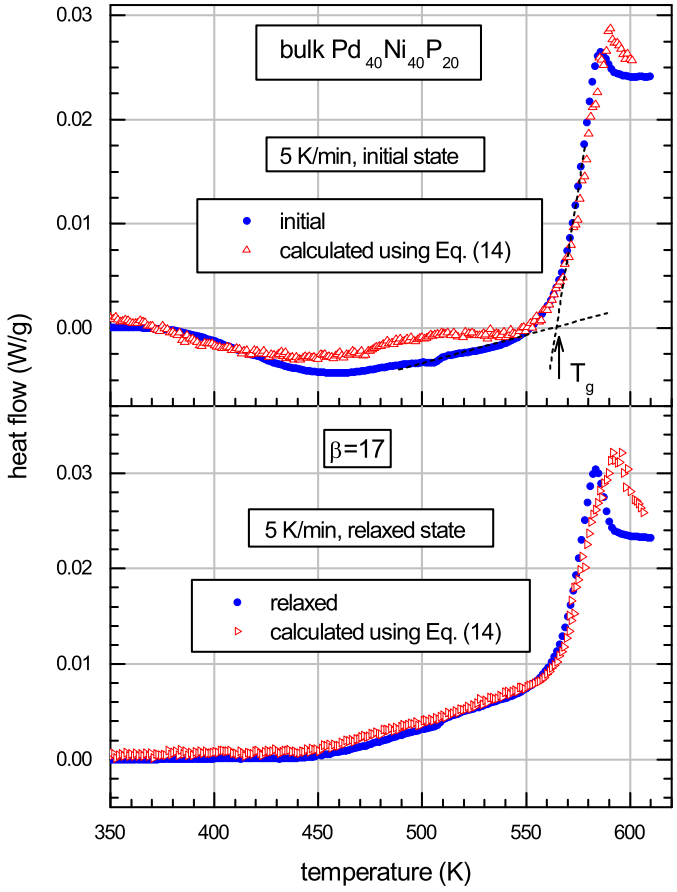

Figure 9. Experimental and calculated DSC thermograms for bulk glassy $Pd_{40}Ni_{40}P_{20}$ in the initial and relaxed states [75]. The calorimetric glass transition temperature is shown by the arrow.

For the relaxed state, the shear modulus $G = G_{rel}$, and Equation (14) determines the corresponding heat flow W_{rel}. Then, the difference between the heat flow in the relaxed and initial states, $\Delta W = W_{rel} - W$, is given by:

$$\Delta W(T) = \frac{\dot{T}}{\beta\rho}\frac{d\Delta G(T)}{dT} \tag{15}$$

where $\Delta G(T) = G(T) - G_{rel}(T)$ is the shear modulus change due to structural relaxation. As discussed above, this change is conditioned by relaxation events with distributed activation energies. Applying the approximation of the characteristic activation energy (see Equation (8) and related description) and using Equation (9), the Expression (15) can be rewritten as:

$$\Delta W(E_0) = \frac{\dot{T} G^{RT} A}{\beta \rho} \frac{d}{dE_0} \frac{\Delta G(E_0)}{G^{RT}} = \frac{\dot{T} G^{RT} A}{\rho} N_0(E_0) \tag{16}$$

From Equation (16), one obtains the formula for the AES [72],

$$N_0(E_0) = \frac{\rho}{\dot{T} A G^{RT}} \Delta W(E_0) \tag{17}$$

Equations (9) and (17) describe the same AES using the data on the shear modulus relaxation and heat flow measured by DSC, respectively. These equations should give, in principle, the same result. The AES calculated from DSC data on the structural relaxation of bulk glassy $Pd_{41.25}Cu_{41.25}P_{17.5}$ is shown in Figure 5 together with the AES determined from independent shear modulus relaxation data. A good correspondence between the two spectra is indeed seen, indicating the self-consistence of the approach under consideration. Similar results were obtained for two other Pd- and Zr-based glasses [72].

Table 1. Parameters of structural relaxation of Pd- and Zr-based glasses [72]: the change of the defect concentration $\Delta c_g = \int n_g(E_0) dE_0$ determined from G-measurements (where n_g is calculated using Equation (9)), the change of the defect concentration $\Delta c_w = \int n_w(E_0) dE_0$ determined from DSC measurements (where n_w is determined using Equation (17)), averaged concentration $\overline{\Delta c} = (\Delta c_g + \Delta c_w)/2$, molar heat of structural relaxation Q_μ (J/mole), number of defects per mole $N_\mu = \overline{\Delta c} N_A$ ($\times 10^{-20}$ mole^{-1}), heat of structural relaxation per defect $Q_d = Q_\mu / N_\mu$ (eV), room-temperature shear modulus G^{RT} (GPa), volume per atom $\Omega = \frac{m_\mu}{\rho N_A}$ ($\times 10^{-29}$ m^3) and interstitialcy formation enthalpy $H = \alpha G \Omega$ (eV).

Glass	Δc_g	Δc_w	$\overline{\Delta c}$	Q_μ	N_μ	Q_d	G^{RT}	Ω	H
$PdCuP$	0.00161	0.00165	0.00163	432	9.8	2.75	32.7	1.33	2.72
$PdNiP$	0.00332	0.00314	0.00323	931	19.5	2.98	38.6	1.28	3.09
$ZrCuAl$	0.00206	0.00220	0.00213	786	12.8	3.84	34.3	1.73	3.71

Table 1 gives interesting comparative data obtained upon analyzing the activation energy spectra for $Pd_{41.25}Cu_{41.25}P_{17.5}$, $Pd_{40}Ni_{40}P_{20}$ and $Zr_{46}Cu_{46}Al_8$ glasses [72]. First, one can calculate the change of the defect concentration during structural relaxation by integrating the spectra determined from measurements of the shear modulus and DSC (*i.e.*, using Equations (9) and (17), respectively). Table 1 shows that both methods of AES reconstruction give very close results. Second, taking the experimental molar heat of structural relaxation Q_μ and calculating the number of defects per mole, $N_\mu = \overline{\Delta c} N_A$, ($\overline{\Delta c}$ is the averaged number of defects annealed out during structural relaxation, N_A the Avogadro number), one can determine the heat of structural relaxation per defect, $Q_d = Q_\mu / N_\mu$. On the other hand, one can calculate the interstitialcy formation enthalpy using Equation (12). Table 1 illustrates a remarkable similarity between the heat of structural relaxation per defect Q_d and interstitialcy formation enthalpy H:

the difference between these quantities is less than 4%. On the other hand, the obtained values of Q_d and H are quite close to the values of the interstitialcy formation enthalpy (2–3 eV) in simple close-packed crystalline metals [29,80]. These arguments constitute further evidence for the interstitialcy-mediated mechanism of structural relaxation.

6. Interstitialcies and Low Temperature Heat Capacity

A fundamental feature of the structural dynamics of glasses of different types consists of the low temperature excess heat capacity, which can be visualized as a peak in the specific heat C divided by the cube of temperature (C/T^3) in the 5 to 15 K temperature range [81]. This peak is called the Boson heat capacity peak. It is commonly accepted that this peak arises from excess vibrational states in glass, which are absent in crystalline materials [81]. There are quite a few approaches derived for the interpretation of the Boson peak (for a review, see [82]), but its physical nature still remains unclear. The Interstitialcy theory considers the Boson peak as originating from low frequency resonance vibration modes of interstitialcies, resulting mainly from excitation to their first excited state [83]. Granato calculated the height H_B of the Boson peak and showed that it is proportional to the concentration c of interstitialcy defects, $H_B = 4.6\frac{c}{0.03}\frac{f}{5}\left(\frac{\omega_0}{7\omega_R}\right)^3$, where f is the number of resonance modes per interstitialcy, ω_D is the Debye frequency and interstitialcy resonance vibration frequencies are assumed to be the same equal to ω_R [83]. The temperature of the Boson peak was calculated as $T_B = \frac{\Theta}{35}\frac{7\omega_R}{\omega_D}$. With a rough estimate, $\frac{7\omega_R}{\omega_D} \approx 1$, this leads to the Boson peak temperature $T_B \approx \frac{\Theta}{35}$, where Θ is the Debye temperature. This gives a reasonable estimate of Boson peak temperature for glasses of various types [83].

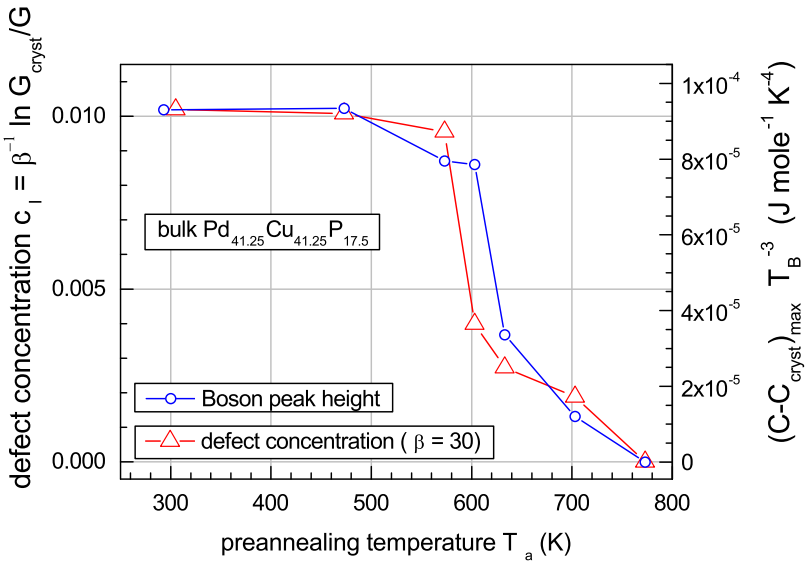

Figure 10. Interstitialcy defect concentration in bulk glassy $Pd_{41.25}Cu_{41.25}P_{17.5}$ calculated using Equation (1) together with the height of the Boson heat capacity peak as a function of the pre-annealing temperature T_a. The curves are drawn as guides for the eye. It is seen that the dependencies of the defect concentration c and Boson peak height on T_a can be superposed, indicating the direct proportionality between them and confirming, thus, the interstitialcy interpretation of the Boson peak [84].

Structural relaxation occurring after annealing at high temperatures below T_g leads to a decrease of the Boson peak height. Simultaneously, the shear modulus increases. The concentration of interstitialcy defects in glass can be estimated using its shear modulus as supposed by Equation (1). It is then possible to compare the defect concentration with the Boson peak height for different pre-annealing temperatures. This program was carried out in [84]. Figure 10 gives the defect concentration together with the Boson peak height (relatively to the crystalline state) in bulk glassy $Pd_{41.25}Cu_{41.25}P_{17.5}$ as a function of pre-annealing temperature T_a. It is seen that both quantities decrease with T_a, as one would expect. After pre-annealing at $T_a = 773\ K$, the glass crystallizes, so that $c = 0$ and the Boson peak disappears. Figure 10 also shows that the dependences of the defect concentration and Boson peak height on T_a can be superposed, indicating the direct proportionality between them and confirming, thus, the understanding of the Boson heat capacity peak on the basis of the Interstitialcy theory (see [84] for more details).

7. Interstitialcies, Free Volume and Enthalpy Release

Most of metallic glasses have smaller density compared to their crystalline counterparts. Since the density is increasing upon structural relaxation of initial MGs below T_g, it is widely believed that elementary structural relaxation events take place in the regions of smaller local density, *i.e.*, in the regions containing some excess "free volume" [4,9,12,13]. In spite of the fact that the "free volume" has no clear theoretical definition, as repeatedly mentioned in the literature (e.g., [17,85]), and the application of this concept to the interpretation of experimental data sometimes leads to evident inconsistencies [16,77], the free volume-based notions still remain quite popular [4,11,15,86]. In this context, it is important to estimate what kind of volume effects could be associated with interstitialcy defects in glass and to compare these with volume effects attributed to the free volume.

For a rough estimate, it can be accepted that the free volume in MGs represents some entity similar to vacancies in crystals, while interstitialcies in MGs are analogous to those in simple metallic crystals. It is known that the insertion of vacancies (v) and interstitialcies (i) gives the volume changes $(\Delta V/\Omega)_v = 1 - \alpha_v$ and $(\Delta V/\Omega)_i = -1 + \alpha_i$, respectively, where Ω is the volume per atom, α_v and α_i are the corresponding relaxation volumes [87]. Then, the resulting relative volume change is $\Delta V/V = (\alpha_v + 1)\, c_v + (\alpha_i - 1)\, c_i$, where c_v and c_i are the concentrations of vacancies and interstitialcies. Granato [87] suggests that $\alpha_v = -0.2$ and $\alpha_i = 2.0$. The calculated values of α_v and α_i for 15 metals given in [29] after averaging are equal to -0.26 and 1.55, respectively, quite close to available experimental data [29,88]. Then, one arrives at $\Delta V/V \approx 0.74c_v + 0.55c_i$, and one has to conclude that the volume effects associated with vacancies and interstitialcies have the same sign and are quite comparable in the magnitude. Therefore, the observed densification of MGs below T_g cannot be solely interpreted as annealing out of the free volume, as pointed out long ago [48]. A decrease of interstitialcy concentration can almost equally lead to the volume contraction.

Isothermal structural relaxation as-cast MGs below T_g leads to a decrease of the volume, which is accompanied by a linear decrease of the molar enthalpy [15]. This dependence is usually interpreted as a result of the free volume decrease [13,15]. However, it was recently shown that this fact can be also understood within the framework of the Interstitialcy theory as a result of a decrease of the interstitialcy

defect concentration. The derivative of the released molar enthalpy H_μ over the relative volume change $\Delta V/V$ then becomes [80]:

$$\frac{dH_\mu}{d\Delta V/V} = -\frac{\alpha m_\mu (1+g) G}{\rho (\alpha_i - 1)} \tag{18}$$

where $\alpha \approx 1$, $g = ln\frac{G}{G_x}$ (G and G_x are the shear moduli of glass and reference crystal) and the volume per atom $\Omega = \frac{m_\mu}{\rho N_A}$, with N_A, m_μ and ρ being the Avogadro number, molar mass and density, respectively. Equation (18) shows that the derivative in the left-hand side should be nearly temperature independent and the released enthalpy should linearly increase with the relative decrease of the volume, in accordance with numerous experimental observations on different MGs [15,80,89]. The estimate of this derivative for an Au-based metallic glass using Equation (18) gives the value of 239 kJ/mol, which is quite close to the experimental value of 187 kJ/mol [80], supporting thus the notions under consideration.

8. Elastic Dipole Approach

The insertion of a defect into a crystal creates local elastic distortions. Because of these distortions, the defect interacts with the applied homogeneous elastic stress. In some sense, this interaction is similar to the interaction of an electric dipole with the applied electric field. Accordingly, the defect, which creates local elastic distortions and interacts with the external stress, is called the "elastic dipole" [90]. The necessary condition for such an interaction consists in the requirement that the symmetry of the defect must be lower than the local symmetry of the matrix structure [90]. This fully applies to dumbbell interstitials, which in fact represent a particular case of elastic dipoles.

In this case, using the conceptual framework described above, one can assume the existence of frozen-in elastic dipoles in glass and accept that they create local anisotropic elastic distortions. This approach was developed in [77,91]. It was shown that: (i) these defects lead to the elastic softening of glass with respect to the reference crystal; and (ii) their stored elastic energy, which is released as heat upon structural relaxation below and above T_g, as well as upon crystallization of glass, closely corresponds to the heat effects observed experimentally. The main points of this approach can be summarized as follows.

The expression for the internal energy U per unit mass of a deformed isotropic body taking into account third- and fourth-order expansion terms was suggested in [92,93] (the same expression was later used in [94]). It is reasonable to assume that the change of the internal energy due to strain-induced dilatation (volume change) is insignificant for MGs [77,91]. Then, the expansion for U has the form [77,91] :

$$\rho U = \rho U_0 + \mu I_2 + \frac{4}{3}\nu_3 I_3 + \frac{1}{2}\gamma_4 I_2^2 \tag{19}$$

where ρ is the density, U_0 the internal energy of the undeformed state, $I_2 = \varepsilon_{ij}\varepsilon_{ji}$ and $I_3 = \varepsilon_{ij}\varepsilon_{jk}\varepsilon_{ik}$ the algebraical invariants of the deformation tensor ε_{ij}, μ the second-order Lamé elastic constants, ν_3 the third-order Lamé elastic constant and γ_3 and γ_4 the fourth-order Lamé elastic constants. If the strain field ε_{ij} in Equation (19) is created by randomly-oriented frozen-in elastic dipoles, then the change of the internal energy ΔU with respect to the reference crystal is:

$$\rho U - \rho U_0 = \rho \Delta U \approx \mu I_2 = \mu c \overline{\lambda_{ij}\lambda_{ji}} \tag{20}$$

where c is the concentration of frozen-in elastic dipoles, λ_{ij} the so-called λ-tensor [90], which characterizes the strain field created by an elastic dipole, and the bar denotes averaging over all elastic dipoles. The components of the λ-tensor are equal to the components of the deformation tensor per unit concentration of unidirectional elastic dipoles [90]. The change of the elastic energy given by Equation (20) is released as heat upon structural relaxation. Then, the heat flow occurring upon warming-up of glass due to the release of the internal energy associated with frozen-in elastic dipoles can be calculated as [77]:

$$W = \frac{\partial \Delta U}{\partial t} = \dot{T}\frac{\partial \Delta U}{\partial T} = \frac{\dot{T}}{\rho}\frac{\partial}{\partial T}\left(\mu c\overline{\lambda_{ij}\lambda_{ji}}\right) \tag{21}$$

With some minor further assumptions, Equation (21) leads to the expression for the heat flow occurring upon warming up of a metallic glass [77],

$$W = \frac{3\dot{T}}{\rho\beta\overline{\Omega}}\left[\frac{dG_x}{dT} - \frac{dG}{dT}\right] \tag{22}$$

where the averaged form-factor $\overline{\Omega} = 1.38$ takes into account different types of elastic dipoles involved in structural relaxation [77]; other quantities have the same meaning as above. The comparison of the heat flow given by this equation with the experimental data taken on glassy $Zr_{46}Cu_{46}Al_8$ revealed their good correspondence [77]. On the other hand, it is to be emphasized that Equation (22) is very similar, although not fully identical, to the heat flow law Equation (14) derived within the framework of the Interstitialcy theory. A detailed comparative analysis of these heat flow laws with the experimental data obtained on glassy $Pd_{41.25}Cu_{41.25}P_{17.5}$ taken as an example was reported in [95]. It was found that both equations quite correctly describe both heat release well below T_g and heat absorption near and above T_g. The elastic dipole approach Equation (22) provides a very good description of heat flow data near and above T_g, but slightly underestimates the heat flow well below T_g. The Interstitialcy theory approach Equation (14) provides a very good description of heat flow data in the whole temperature range. It is clear that the heat flow is conditioned by the relaxation of the shear modulus, as implied by both Equations (14) and (22).

Since the difference in the heat flow given by Equations (14) and (22) is small, one can derive the relationship between the shear susceptibilities entering these formulae. Designating the shear susceptibilities in Equations (14) and (22) as β_i and β_d, respectively, taking into account that the expressions in square brackets of these equations are approximately equal, one arrives at $\beta_i \approx \frac{1}{3}\overline{\Omega}\beta_d$. Fitting to the calorimetric data for $Pd_{41.25}Cu_{41.25}P_{17.5}$ glass gives $\beta_d = 38$ (just the same value as for glassy $Zr_{46}Cu_{46}Al_8$ [77]). Then, with the above relationship and $\overline{\Omega} = 1.38$, one calculates $\beta_i = 17.5$, which is quite close to $\beta_i = 20$ derived by fitting to the calorimetric data for the same glass [95].

The elastic dipole approach sketched above gives clear information on the reason for the shear softening of glass with respect to the reference crystal. The expression for the shear modulus of glass can be written down as [77,91]:

$$G = \mu + \gamma_4\Omega_t c\overline{\lambda_{ij}\lambda_{ji}} \tag{23}$$

where Ω_t is the averaged dipole form factor for the shear deformation. If the defect concentration $c = 0$, the quantity μ equals the shear modulus G_x of the reference crystal. The only metallic glass for which

the fourth-rank modulus γ_4 is so far known is $Zr_{52.5}Ti_5Cu_{17.9}Ni_{14.6}Al_{10}$ [93]. With $\gamma_4 = -171$ GPa and other estimates for this glass, $c \approx 0.039$ and $\overline{\lambda_{ij}\lambda_{ji}} = 0.92 \pm 0.12$ [91], Equation (23) gives $\Delta G = G_x - G \approx 8.0$ GPa, fairly close to the experimental value $\Delta G \approx 9.3$ GPa [91], supporting thus the elastic dipole approach.

It is important to emphasize that the elastic constants ν_3 and γ_4 in the non-linear expansion Equation (19) for the internal energy are essentially anharmonic (in the harmonic approximation, these constants are equal to zero). Since G is determined by γ_4 (see Equation (23)), one has to conclude that the shear softening of MGs with respect to the reference crystalline state is determined by the anharmonicity of the interatomic potential.

The same conclusion immediately comes from the Interstitialcy theory. Indeed, the shear susceptibility in the main Equation (1) constitutes a major parameter, which is defined as $\beta = -\frac{1}{G}\frac{\partial^2 G}{\partial \varepsilon^2}$ (ε is the shear strain) [18]. The shear susceptibility is non-zero only if the non-linear elasticity is taken into account. A similar definition of β is considered in the elastic dipole approach, which directly gives the linear proportionality between the shear susceptibility and the absolute value of γ_4 elastic constant, $\beta = -\frac{3\gamma_4}{G}$ [77]. The understanding that non-linear elastic effects occurring due to the anharmonicity of the interatomic potential are manifested in many of MGs' properties has now been increasing [59,96–101]. In particular, the role of non-linear elastic effects in the mechanical behavior of metallic glasses at high stresses seems to be quite evident [94,102,103].

9. Summary

The Interstitialcy theory provides a new comprehensive, versatile and verifiable approach to the understanding of the structural relaxation of metallic glasses. This approach starts with the assumption that melting of simple metallic crystals takes place as a result of rapid multiplication of dumbbell (split) interstitials (= interstitialcies). The nucleus of such a defect can be interpreted as two atoms trying to occupy the same minimum of the potential energy. On the other hand, these defects create internal stresses interacting with the external stress and can be considered as elastic dipoles. In the liquid state, the defects retain their individuality, but become inherent structural elements, rather than "defects" of the structure. Rapid melt quenching partially freezes the interstitialcy defect structure in solid glass. Heat treatment of the glass leads to a change of the interstitialcy defect concentration, which can be precisely monitored by measurements of the shear modulus. The latter represents the major physical quantity controlling the relaxation kinetics through the main Equation (1) of the Interstitialcy theory.

The sign of structural relaxation monitored by measurements of the shear modulus is conditioned by current temperature and glass thermal prehistory that results in a different relations between the current interstitialcy defect concentration, c, and the defect concentration in the metastable equilibrium, c_{eq}. At temperatures far below T_g, usually $c > c_{eq}$ and the relaxation lead to a decrease of c, with a corresponding increase of the shear modulus. Near and above T_g, c can be smaller than c_{eq}, leading to a decrease of the shear modulus. It has been found that the Interstitialcy theory provides a good description of the relaxation kinetics for different metallic glasses and testing conditions.

The basic Equation (1) of the Interstitialcy theory establishes the direct relationship between the shear modulus of glass, the concentration of frozen-in interstitialcy defects and the shear modulus

of the maternal crystal. It has been revealed that this relationship conforms with the available experimental data. In particular, when structural relaxation is absent, Equation (1) implies the equality of temperature coefficients of the shear moduli in the glassy and crystalline states (Equation (11)), which is proved experimentally.

Any change of the interstitialcy concentration alters the elastic energy associated with them. If c decreases upon structural relaxation, the stored elastic energy is released as heat. Increasing c requires an augmentation of the external energy, which is manifested as heat absorption. The Interstitialcy theory leads to the general heat flow law Equation (14), which directly states that the heat effects occurring upon heating are controlled by the relaxation of the shear modulus, while the underlying physical reason consists of the relaxation of the internal interstitialcy defect system. It has been found that this law correctly describes exothermal heat flow well below T_g, as well as endothermal heat reaction near and above T_g.

The Interstitialcy theory provides two independent ways for the reconstruction of the activation energy spectrum of atomic rearrangements occurring upon structural relaxation. The first of them (Equation (9)) is based on shear modulus relaxation data, while the second one (Equation (17)) makes use of heat flow data. It has been found that both methods give nearly the same results, and the formation energy of defects responsible for structural relaxation is close to the interstitialcy formation energy implied by the Interstitialcy theory (Equation (12)).

It has been found that the height of the low temperature Boson heat capacity peak strongly correlates with the changes in the shear modulus upon high temperature annealing. The Interstitialcy theory connects this peak with low frequency resonant localized vibrations of interstitialcy defects frozen-in upon glass production. The height of this peak is proportional to the defect concentration and, together with the peak temperature, reasonably agrees with the experiment.

Since dumbbell interstitials are in fact elastic dipoles, it is possible to develop a more general approach based on the non-linear theory of elasticity. This approach gives nearly the same expression (Equation (22)) for structural relaxation-induced heat flow and makes clear evidence that the heat effects, as well as the shear softening of metallic glasses are intrinsically connected with the anharmonicity of the interatomic interaction.

Acknowledgments

The author is cordially grateful to Professor A.V. Granato for many inspiring discussions and fruitful cooperation over the years. Long-term collaboration with D.M. Joncich (University of Illinois at Urbana-Champaign, IL, USA), N.P. Kobelev (Institute for Solid State Physics, Chernogolovka, Russian Academy of Sciences), Yu.P. Mitrofanov, R.A. Konchakov, G.V. Afonin and A.S. Makarov (State Pedagogical University, Voronezh, Russia) is kindly acknowledged. The support for this work was provided by the Ministry of Education and Science of the Russian Federation (Project 3.114.2014/K).

Conflicts of Interest

The author declares no conflict of interest.

References

1. Taub, A.I.; Spaepen, F. Isoconfigurational flow of amorphous $Pd_{82}Si_{18}$. *Scr. Metall.* **1979**, *13*, 195–198.
2. Khonik, V.A. The kinetics of irreversible structural relaxation and rheological behavior of metallic glasses under quasi-static loading. *J. Non-Cryst. Sol.* **2001**, *296*, 147–157.
3. Chen, H.S. Glassy metals. *Rep. Prog. Phys.* **1980**, *43*, 353–432.
4. Schuh, C.A.; Hufnagel, T.C.; Ramamurty, U. Mechanical behavior of amorphous alloys. *Acta Mater.* **2007**, *55*, 4067–4109.
5. Greer, A.L. Metallic Glasses. In *Physical Metallurgy*; Volume I; Laughlin, D.E., Hono, K., Eds.; Elsevier: Oxford, UK, 2014; pp. 305–385.
6. Doolittle, A.K. Studies in newtonian flow. II. The dependence of the viscosity of liquids on free-space. *J. Appl. Phys.* **1951**, *22*, 1471–1475.
7. Turnbull, D.; Cohen, M.H. Free volume model of the amorphous phase: glass transition. *J. Chem. Phys.* **1961**, *34*, 120–125.
8. Turnbull, D.; Cohen, M.H. On the free volume model of the liquid-glass transition. *J. Chem. Phys.* **1970**, *52*, 3038–3041.
9. Spaepen, F. A microscopic mechanism for steady state inhomogeneous flow in metallic glasses. *Acta Metall.* **1977**, *25*, 407–415.
10. Argon, A.S. Plastic deformation in metallic glasses. *Acta Metall.* **1979**, *27*, 47–58.
11. Spaepen, F. Homogeneous flow of metallic glasses: A free volume perspective. *Scr. Mater.* **2006**, *54*, 363–367.
12. Van den Beukel, A.; Radelaar, S. On the kinetics of structural relaxation in metallic glasses. *Acta Metall.* **1990**, *31*, 419–427.
13. Van den Beukel, A.; Sietsma, J. The glass transition as a free volume related kinetic phenomenon. *Acta Metall. Mater.* **1990**, *38*, 383–389.
14. Koebrugge, G.W.; Sietsma, J.; van den Beukel, A. Structural relaxation in amorphous $Pd_{40}Ni_{40}P_{20}$. *Acta Metall. Mater.* **1992**, *40*, 753–760.
15. Slipenyuk, A.; Eckert, J. Correlation between enthalpy change and free volume reduction during structural relaxation of $Zr_{55}Cu_{30}Al_{10}Ni_5$ metallic glass. *Scr. Mater.* **2004**, *50*, 39–44.
16. Bobrov, O.P.; Khonik, V.A.; Lyakhov, S.A.; Csach, K.; Kitagawa, K.; Neuhäuser, H. Shear viscosity of bulk and ribbon glassy $Pd_{40}Cu_{30}Ni_{10}P_{20}$ well below and mear the glass transition. *J. Appl. Phys.* **2006**, *100*, 033518.
17. Cheng, Y.Q.; Ma, E. Indicators of internal structural states for metallic glasses: Local order, free volume, and configurational potential energy. *Appl. Phys. Lett.* **2008**, *93*, 051910.
18. Granato, A.V. Interstitialcy model for condensed matter states of face-centered-cubic metals. *Phys. Rev. Lett.* **1992**, *68*, 974–977.
19. Granato, A.V. Interstitialcy theory of simple condensed matter. *Eur. J. Phys.* **2014**, *87*, 18.
20. Frenkel, J. *Kinetic Theory of Liquids*; Oxford University Press: New York, NY, USA, 1946.
21. Mei, Q.S.; Lu, K. Melting and superheating of crystalline solids: From bulk to nanocrystals. *Prog. Mater. Sci.* **2007**, *52*, 1175–1262.

22. Slater, J.C. *Introduction to Chemical Physics*; McGraw-Hill Book Company: New York, NY, USA; Toronto, ON, Canada; London, UK, 1963.
23. Granato, A.V. A comparison with empirical results of the Interstitialcy theory of condensed matter. *J. Non-Cryst. Sol.* **2006**, *352*, 4821–4825.
24. Seitz, F. On the theory of diffusion in metals. *Acta Cryst.* **1950**, *3*, 355–363.
25. Gibson, J.B.; Goland, A.N.; Milgram, M.; Vineyard, G.H. Dynamics of radiation damage. *Phys. Rev.* **1960**, *120*, 1229–1253.
26. Erginsoy, C.; Vineyard, G.H.; Englert, A. Dynamics of radiation damage in a body-centered cubic lattice. *Phys. Rev.* **1964**, *133*, A595–A606.
27. Schilling, W. Self-interstitial atoms in metals. *J. Nucl. Mater.* **1978**, *69–70*, 465–489.
28. Robrock, K.H. *Mechanical Relaxation of Interstitials in Irradiated Metals*; Springer-Verlag: Berlin, Germany, 1990.
29. Wolfer, W.G. Fundamental Properties of Defects in Metals. In *Comprehensive Nuclear Materials*; Konings, R.J.M., Ed.; Elsevier: Amsterdam, The Netherlands, 2012.
30. Konchakov, R.A.; Khonik, V.A.; Kobelev, N.P. Split Interstitials in computer models of single-crystal and amorphous copper. *Phys. Sol. State* (*Pleiades Publishing*) **2015**, *57*, 844–852.
31. Holder, J.; Granato, A.V.; Rehn, L.E. Experimental evidence for split interstitials in copper. *Phys. Rev. Lett.* **1974**, *32*, 1054–1057.
32. Holder, J.; Rehn, L.E.; Granato, A.V. Effect of self-interstitials on the elastic constants of copper. *Phys. Rev. B* **1974**, *10*, 363–375.
33. Born, M. Thermodynamics of crystals and melting. *J. Chem. Phys.* **1939**, *7*, 591–603.
34. Dederichs, P.H.; Lehman, C.; Schober, H.R.; Scholz, A.; Zeller, R. Lattice theory of point defects. *J. Nucl. Mater.* **1978**, *69–70*, 176–199.
35. Nordlund, K.; Averback, R.S. Role of self-interstitial atoms on the high temperature properties of metals. *Phys Rev. Lett.* **1998**, *80*, 4201–4204.
36. Spaepen, F. A survey of energies in materials science. *Phil. Mag.* **2005**, *85*, 2979–2987.
37. De Podesta, M. *Understanding the Properties of Matter*, 2nd ed.; Taylor & Francis: London, UK, 2001.
38. Nordlund, K.; Ashkenazy, Y.; Averback, R.S.; Granato, A.V. Strings and interstitials in liquids, glasses and crystals. *Europhys. Lett.* **2005**, *71*, 625–631.
39. Granato, A.V.; Joncich, D.M.; Khonik, V.A. Melting, thermal expansion, and the Lindemann rule for elemental substances. *Appl. Phys. Lett.* **2010**, *97*, 171911.
40. Stillinger, F.H.; Weber, T.A. Point defects in bcc crystals: Structures, transition kinetics, and melting implications. *J. Chem. Phys.* **1984**, *81*, 5095–51034.
41. Lee, G.C.S.; Li, J.C.M. Molecular-dynamics studies of crystal defects and melting. *Phys. Rev. B* **1989**, *39*, 9302–9311.
42. Kanigel, A.; Adler, J.; Polturak, E. Influence of point defects on the shear elastic coefficients and on the melting temperature of copper. *Int. J. Mod. Phys. C* **2001**, *12*, 727–737.
43. Zhang, H.; Khalkhali, M.; Liu, Q.; Douglas, J.F. String-like cooperative motion in homogeneous melting. *J. Chem. Phys.* **2013**, *138*, 12A538.

44. Ashkenazy, Y.; Averback, R.S. Atomic mechanisms controlling crystallization behavior in metals at deep undercoolings. *Europhys. Lett.* **2007**, *79*, 26005.
45. Betancourt B.A.P.; Douglas, J.F.; Starr, F.W. String model for the dynamics of glass-forming liquids. *J. Chem. Phys.* **2014**, *140*, 204509.
46. Schober, H.R. Collectivity of motion in undercooled liquids and amorphous solids. *J. Non-Cryst. Sol.* **2002**, *307-310*, 40–49.
47. Donati, C.; Douglas, J.F.; Kob, W.; Plimpton, S.J.; Poole, P.H.; Glotzer, S.C. Stringlike cooperative motion in a supercooled liquid. *Phys. Rev. Lett.* **1998**, *80*, 2338–2341.
48. Oligschleger, C.; Schober, H.R. Collective jumps in a soft-sphere glass. *Phys. Rev. B* **1999**, *59*, 811–821.
49. Granato, A.V. The specific heat of simple liquids. *J. Non-Cryst. Sol.* **2002**, *307–310*, 376–386.
50. Konchakov, R.A.; Khonik, V.A. Effect of vacancies and interstitials in the dumbbell configuration on the shear modulus and vibrational density of states of copper. *Phys. Sol. State* (*Pleiades Publishing*) **2014**, *56*, 1368–1373.
51. Schober H.R. *Phonons 89*; Hunklinger, S., Ludwig, W., Weiss, G., Eds.; World Scientific: Singapore, 1989; Volume I, p. 444.
52. Okamoto, P.R.; Rehn, L.E.; Pearson, J.; Bhadra, R.; Grimsditch, M. Brillouin scattering and transmission electron microscopy studies of radiation-induced elastic softening, disordering and amorphization of metallic compounds. *J. Less-Common Met.* **1988**, *14*, 231–244.
53. Landau, L.D.; Lifshitz, E.M. *Theory of Elasticity*; Pergamon Press: Oxford, UK, 1970.
54. Nemilov, S.V. The kinetics of elementary processes in the condensed state. II. Shear relaxation and the equation of state for solids. *Russ. J. Phys. Chem.* **1968**, *42*, 726–731.
55. Dyre, J.C.; Olsen, N.B.; Christensen, T. Local elastic expansion model for viscous-flow activation energies of glass-forming molecular liquids. *Phys. Rev. B* **1996**, *53*, 2171–2174.
56. Johnson, W.L.; Samwer, K. A universal criterion for plastic yielding of metallic glasses with a $(T/T_g)^{2/3}$ temperature dependence. *Phys Rev. Lett.* **2005**, *95*, 195501.
57. Nemilov, S.V. Interrelation between shear modulus and the molecular parameters of viscous flow for glass forming liquids. *J. Non-Cryst. Sol.* **2006**, *352*, 2715–2725.
58. Dyre, J.C. The glass transition and elastic models of glass-forming liquids. *Rev. Mod. Phys.* **2006**, *78*, 953–972.
59. Wang, W.H. The elastic properties, elastic models and elastic perspertives of metallic glasses. *Prog. Mater. Sci.* **2012**, *57*, 487–656.
60. Tsao, S.S.; Spaepen, F. Structural relaxation of a metallic glass near equilibrium. *Acta Metall.* **1985**, *33*, 881–889.
61. Mitrofanov, Yu.P.; Khonik, V.A.; Granato, A.V.; Joncich, D.M.; Khonik, S.V.; Khoviv, A.M. Relaxation of a metallic glass to the metastable equilibrium: Evidence for the existence of the Kauzmann pseudocritical temperature. *Appl. Phys. Lett.* **2012**, *100*, 171901.
62. Khonik, V.A.; Mitrofanov, Y.P.; Makarov, A.S.; Konchakov, R.A.; Afonin, G.V.; Tsyplakov, A.N. Structural relaxation and shear softening of Pd- and Zr-based bulk metallic glasses near the glass transition. *J. Alloys Comp.* **2015**, *628*, 27–31.

63. Khonik, V.A.; Mitrofanov, Y.P.; Khonik, S.V.; Saltykov, S.N. Unexpectedly large relaxation time determined by in situ high-frequency shear modulus measurements near the glass transition of bulk glassy $Pd_{40}Cu_{30}Ni_{10}P_{20}$. *J. Non-Cryst. Sol.* **2010**, *356*, 1191–1193.
64. Gibbs, M.R.J.; Evetts, J. E.; Leake, J.A. Activation energy spectra and relaxation in amorphous materials. *J. Mater. Sci.* **1983**, *18*, 278–288.
65. Wagner, H.; Bedorf, D.; Küchemann, S.; Schwabe, M.; Zhang, B.; Arnold, W.; Samwer, K. Local elastic properties of a metallic glass. *Nat. Mater.* **2011**, *10*, 439–442.
66. Khonik, V.A. The kinetics of irreversible structural relaxation and homogeneous plastic flow of metallic glasses. *Phys. Status Sol. (A)* **2000**, *177*, 173–189.
67. Khonik, S.V.; Granato, A.V.; Joncich, D.M.; Pompe, A.; Khonik, V.A. Evidence of distributed interstitialcy-like relaxation of the shear modulus due to structural relaxation of metallic glasses. *Phys. Rev. Lett.* **2008**, *100*, 065501.
68. Bothe, K.; Neuhäuser, H. Relaxation of metallic glass structure measured by elastic modulus and internal friction. *J. Non-Cryst. Sol.* **1983**, *56*, 279–284.
69. Mitrofanov, Yu.P.; Khonik, V.A.; Vasil'ev, A.N. Isothermal kinetics and relaxation recovery of high-frequency shear modulus in the course of structural relaxation of $Pd_{40}Cu_{30}Ni_{10}P_{20}$ bulk glass. *J. Exp. Theor. Phys.* **2009**, *108*, 830–835.
70. Mitrofanov, Yu.P.; Khonik, V.A.; Granato, A.V.; Joncich, D.M.; Khonik, S.V. Relaxation of the shear modulus of a metallic glass near the glass transition. *J. Appl. Phys.* **2011**, *109*, 073518.
71. Khonik, V.A.; Kitagawa, K.; Morii, H. On the determination of the crystallization activation energy of metallic glasses. *J. Appl. Phys.* **2000**, *87*, 8440–8443.
72. Tsyplakov, A.N.; Mitrofanov, Yu.P.; Makarov, A.S.; Afonin, G.V.; Khonik, V.A. Determination of the activation energy spectrum of structural relaxation in metallic glasses using calorimetric and shear modulus relaxation data. *J. Appl. Phys.* **2014**, *116*, 123507.
73. Makarov, A.S. Khonik, V.A.; Mitrofanov, Yu.P.; Granato, A.V.; Joncich, D.M.; Khonik, S.V. Interrelationship between the shear modulus of a metallic glass, concentration of frozen-in defects, and shear modulus of the parental crystal. *Appl. Phys. Lett.* **2013**, *102*, 091908.
74. Khonik, V.A.; Mitrofanov, Yu.P.; Lyakhov, S.A.; Khoviv, D.A.; Konchakov, R.A. Recovery of structural relaxation in aged metallic glass as determined by high-precision in situ shear modulus measurements. *J. Appl. Phys.* **2009**, *105*, 123521.
75. Makarov, A.S.; Khonik, V.A.; Wilde, G.; Mitrofanov, Yu.P.; Khonik, S.V. "Defect"-induced heat flow and shear modulus relaxation in a metallic glass. *Intermetallics* **2014**, *44*, 106–109.
76. Makarov, A.S.; Mitrofanov, Yu.P.; Afonin, G.V.; Khonik, V.A.; Kobelev, N.P. The dependence of the shear modulus of glass on the shear modulus of crystal and kinetics of structural relaxation for $Zr_{46}Cu_{46}Al_8$ system. *Phys. Sol. State* (*Pleiades Publishing*) **2015**, *57*, in press.
77. Kobelev, N.P.; Khonik, V.A.; Makarov, A.S.; Afonin, G.V.; Mitrofanov, Yu.P. On the nature of heat effects and shear modulus softening in metallic glasses: A generalized approach. *J. Appl. Phys.* **2014**, *115*, 033513.
78. Mitrofanov, Yu.P.; Makarov, A.S.; Khonik, V.A.; Granato, A.V.; Joncich, D.M.; Khonik, S.V. On the nature of enthalpy relaxation below and above the glass transition of metallic glasses. *Appl. Phys. Lett.* **2012**, *101*, 191903.

79. Makarov, A.S.; Khonik, V.A.; Mitrofanov, Yu.P.; Granato, A.V.; Joncich, D.M. Determination of the susceptibility of the shear modulus to the defect concentration in a metallic glass. *J. Non-Cryst. Sol.* **2013**, *370*, 18–20.
80. Khonik, V.A.; Kobelev, N.P. Alternative understanding for the enthalpy *vs.* volume change upon structural relaxation of metallic glasses. *J. Appl. Phys.* **2014**, *115*, 093510.
81. Phillips, W.A. *Amorphous Solids: Low Temperature Properties*; Springer: Berlin, Germany, 1981.
82. Shintani, H.; Tanaka, H. Universal link between the boson peak and transverse phonons in glass. *Nat. Mater.* **2008**, *7*, 870–877.
83. Granato, A.V. Interstitial resonance modes as a source of the boson peak in glasses and liquids. *Phys. B* **1996**, *219–220*, 270–272.
84. Vasiliev, A.N.; Voloshok, T.N.; Granato, A.V.; Joncich, D.M.; Mitrofanov, Yu.P.; Khonik, V.A. Relationship between low-temperature boson heat capacity peak and high-temperature shear modulus relaxation in a metallic glass. *Phys. Rev. B* **2009**, *80*, 172102.
85. Miracle, D.B.; Egami, T.; Flores, K.M.; Kelton, K.F. Structural aspects of metallic glasses. *MRS Bull.* **2007**, *32* 629–634.
86. Trexler, M.M.; Thadhani, N.N. Mechanical properties of bulk metallic glasses. *Prog. Mater. Sci.* **2010**, *55*, 759–839.
87. Gordon, C.A.; Granato, A.V.; Simmons, R.O. Evidence for the self-interstitial model of liquid and amorphous states from lattice parameter measurements in krypton. *J. Non-Cryst. Sol.* **1996**, *205–207*, 216–220.
88. Ehrhart, P. Jung, P.; Schultz, H.; Ullmaier, H. Properties and Interactions of Atomic Defects in Metals and Alloys. In *Atomic Defects in Metals, Landolt-Börnstein New Series III*; Madelung, O., Ed.; Springer: Berlin, Germany, 1991; Volume 25, pp. 88–371.
89. Bünz, J.; Wilde, G. Direct measurement of the kinetics of volume and enthalpy relaxation of an Au-based metallic glass. *J. Appl. Phys.* **2013**, *114*, 223503.
90. Nowick, A.S.; Berry, B.S. *Anelastic Relaxation in Crystalline Solids*; Academic Press: New York, NY, USA, 1972.
91. Kobelev, N.P.; Khonik, V.A.; Afonin, G.V.; Kolyvanov, E.L. On the origin of the shear modulus change and heat release upon crystallization of metallic glasses. *J. Non-Cryst. Sol.* **2015**, *411*, 1–4.
92. Erofeyev, V.I. *Wave Processes in Solids With Microstructure*; World Scientific: Singapore, 2003.
93. Kobelev, N.P.; Kolyvanov, E.L.; Khonik, V.A. Higher order elastic moduli of the bulk metallic glass $Zr_{52.5}Ti_5Cu_{17.9}Ni_{14.6}Al_{10}$. *Phys. Sol. State* (*Pleiades Publishing*) **2007**, *49*, 1209–1215.
94. Nakamura, A.; Kamimura, Y.; Edagawa, K.; Takeuchi, S. Elastic and plastic characteristics of a model Cu-Zr amorphous alloy. *Mater. Sci. Eng.* **2014**, *A614*, 16–26.
95. Tsyplakov, A.N.; Mitrofanov, Yu.P.; Khonik, V.A.; Kobelev, N.P.; Kaloyan, A.A. Relationship between the heat flow and relaxation of the shear modulus in bulk PdCuP metallic glass. *J. Alloys Comp.* **2015**, *618*, 449–454.

96. Lambson, E.F.; Lambson, W.A.; Macdonald, J.E.; Gibbs, M.R.J.; Saunders, G.A.; Turnbull, D. Elastic behavior and vibrational anharmonicity of a bulk $Pd_{40}Ni_{40}P_{20}$ metallic glass. *Phys. Rev. B* **1986**, *33*, 2380–2385.
97. Wang, R.J.; Wang, W.H.; Li, F.Y.; Wang, L.M.; Zhang, Y.; Wen, P.; Wang, J.F. The Grüneisen parameter for bulk amorphous materials. *J. Phys.: Condens. Matter* **2003**, *15*, 603–608.
98. Novikov, V.N.; Sokolov, A.P. Poisson ratio and the fragility of glass-forming liquids. *Nature* **2004**, *431*, 961–963.
99. Tarumi, R.; Hirao, M.; Ichitsubo, T.; Matsubara, E.; Saida, J.; Kato, H. Low-temperature acoustic properties and quasiharmonic analysis for Cu-based bulk metallic glasses. *Phys. Rev. B* **2007**, *76*, 104206.
100. Safarik, D.J.; Schwarz, R.B. Evidence for highly anharmonic low-frequency vibrational modes in bulk amorphous $Pd_{40}Cu_{40}P_{20}$. *Phys. Rev. B* **2009**, *80*, 094109.
101. Chen, L.Y.; Li, B.Z.; Wang, X.D.; Jiang, F.; Ren, Y.; Liaw, P.K.; Jiang, J.Z. Atomic-scale mechanisms of tension–compression asymmetry in a metallic glass. *Acta Mater.* **2013**, *61*, 1843–1850.
102. Wang, H.; Li, M. Symmetry breaking and other nonlinear elastic responses of metallic glasses subject to uniaxial loading. *J. Appl. Phys.* **2013**, *113*, 213515.
103. Wang, H.; Li, M. Estimate of the maximum strength of metallic glasses from finite deformation theory. *Phys. Rev. Lett.* **2013**, *111*, 065507.